CONFIDENTIAL

Copy 528
RM H57C22

NACA RM H57C22

NACA

RESEARCH MEMORANDUM

FLIGHT-DETERMINED INDUCTION-SYSTEM AND SURGE CHARACTERISTICS OF THE YF-102 AIRPLANE WITH A TWO-SPOOL TURBOJET ENGINE

By Edwin J. Saltzman

High-Speed Flight Station
Edwards, Calif.

Classification Changed to Unclassified
Authority: NASA Technical Publications Announcements No. 33
Effective Date: October 28, 1960 WHL

CLASSIFIED DOCUMENT

This material contains information affecting the National Defense of the United States within the meaning of the espionage laws, Title 18, U.S.C., Secs. 793 and 794, the transmission or revelation of which in any manner to an unauthorized person is prohibited by law.

NATIONAL ADVISORY COMMITTEE
FOR AERONAUTICS

WASHINGTON

June 28, 1957

CONFIDENTIAL

NATIONAL ADVISORY COMMITTEE FOR AERONAUTICS

RESEARCH MEMORANDUM

FLIGHT-DETERMINED INDUCTION-SYSTEM AND SURGE CHARACTERISTICS OF THE YF-102 AIRPLANE WITH A TWO-SPOOL TURBOJET ENGINE

By Edwin J. Saltzman

SUMMARY

A brief compressor-surge and pressure-recovery program has been completed for the Convair YF-102 airplane with a two-spool turbojet engine. The study covered an altitude range from about 33,000 to 50,000 feet and a Mach number range from 0.6 to 1.1.

The results indicate that this induction system-engine combination had low compressor-surge incidence for normal-flight operations and that there was no relationship between distortion at the compressor face and the surges encountered. In addition, it was found that, for the range of these tests, distortion was not related to angle of attack, sideslip, or free-stream Mach number. This is probably due to the natural mixing associated with the low expansion angle of the diffuser. However, there was a relationship between distortion and normalized air-flow rate. Duct internal-recovery losses were quite high because the duct-engine system was mismatched for most flight conditions. These internal losses were not affected by angle of attack or free-stream Mach number; however, inlet lip losses increased rapidly with angle of attack. This increase is greatly aggravated when Mach number exceeds 1.0. It was found that the total-pressure variation with angle of attack for the YF-102 twin-side inlet system is not the same on both sides and varies in a repeatable manner.

INTRODUCTION

The problem of compressor surge has been encountered recently during flights of turbojet-powered high-speed airplanes. Compressor surge is the condition wherein most of the compressor blades stall simultaneously, permitting the high-pressure gases in the combustion chamber to flow toward the inlet duct. Many surges are accompanied by a loud report and flames may be forced through the duct.

In the past it has been thought that compressor surges occurred under conditions where there was a wide variation in total pressure across the compressor face caused by a poor inlet configuration. During wind-tunnel tests to establish surge conditions for an engine, it is difficult to simulate the effects of changes in angle of attack and sideslip encountered in flight. It was decided, therefore, to measure the pressure profiles at the compressor face during flight tests of fighter- and interceptor-type airplanes at the NACA High-Speed Flight Station, at Edwards, Calif.

This paper presents the results of such tests made on the Convair YF-102 airplane equipped with a twin-side inlet duct system and a two-spool turbojet engine. Some compressor surges were encountered during these tests and an attempt is made to relate surge occurrence with compressor face conditions. The data were obtained at altitudes from 33,000 to 50,000 feet and over the Mach number range from 0.6 to 1.1.

SYMBOLS

A	cross-sectional area, sq ft
A_s	duct skin area, sq ft
h_p	pressure altitude, ft
M	Mach number
m/m_0	mass-flow ratio, $\frac{\text{Duct mass flow}}{\rho_0 V_0 A_{inlet}}$
N_{high}	inboard compressor speed (high speed), rpm
N_{low}	outboard compressor speed (low speed), rpm
p'	total pressure, lb/sq ft
r	radial segment
T'	air total temperature, $^{\circ}R$
V	velocity, ft/sec
w_a	air-flow rate, lb/sec

$\frac{w_a\sqrt{\theta_c}}{\delta_c}$ air-flow rate normalized to sea-level conditions, lb/sec

α angle of attack, deg

β angle of sideslip, deg

Δ_{max} maximum distortion factor, $\frac{p'_{l_{max}} - p'_{l_{min}}}{p'_{l_{av}}}$

Δ_{av} distortion factor, average absolute deviation in percent of average pressure recovery,

$$\frac{\Sigma|\delta|100}{n\left(\frac{p'_l}{p'_0}\right)_{av}}$$

where

$$\delta = \frac{p'_l}{p'_0} - \left(\frac{p'_l}{p'_0}\right)_{av}$$

and n = number probes

δ_c altitude normalizing factor, $\frac{p'}{2116}$

θ compressor face circumferential station, deg

θ_c temperature normalizing factor, $\frac{T'}{518.4^\circ\ R}$

ρ density of air, slugs/cu ft

Subscripts:

0 free stream

3 compressor face station

l	local
av	average
max	maximum
min	minimum
L	left
R	right

AIRPLANE

The Convair YF-102 airplane is a single-engine, 60° delta-wing interceptor powered by a two-spool turbojet engine having an installed sea-level thrust of about 11,300 pounds with afterburner or 7,400 pounds without afterburner. Air is supplied to the engine through two side inlets which join immediately ahead of the compressor face. A photograph of the airplane (fig. 1) shows the inlet shape and location. Additional physical details are described in reference 1.

SURVEY STATIONS AND INSTRUMENTATION

Pressure surveys were made at five stations spaced longitudinally along the inlet-propulsion system. Survey station 1 in the duct of the YF-102 airplane was located immediately aft of the inlet, station 2 about 5 feet aft of the inlet, and station 3 ahead of the compressor face. Photographs of these stations including the survey rakes are shown in figure 2. The types of rakes used are shown in more detail in figure 3. Insensitivity to flow angularity, for probes at stations 1, 2, and 3, is assured by internal chamfering of the leading-edge to a 30° included angle. Support structure influences are minimized by limiting rake width to about 28 percent of probe length. The rakes at stations 1 and 2 average the pressures from all total-pressure probes. At station 3, however, the pressure for each probe is recorded individually. The rakes at the intercompressor and compressor discharge stations (4 and 5) consisted of several radially distributed probes which were connected to a common recording cell. These rakes (stations 4 and 5) were designed and built especially for the engine by the manufacturer. The locations of each of these stations relative to one another are shown in figure 4, along with other pertinent physical details.

Total and static pressure in the duct and at the compressor face and total pressure at the compressor discharge were measured with NACA 12-cell manometers; a pressure transducer was used at the intercompressor station. Total air temperature was measured by a shielded resistance-type probe located beneath the fuselage nose. Total temperature T'_3 was assumed to be the same as free-stream total temperature. An NACA standard airspeed head provided free-stream total and static pressure from points about 90 and 80 inches, respectively, ahead of the fuselage zero length station.

The YF-102 airplane contained standard NACA instruments and synchronizing timer for recording general flight data pertinent to the program.

ACCURACY

It is estimated that the instrument errors involved in measuring total and static pressure in the duct are about ±5 lb/sq ft; however, the installation error in static pressure is uncertain, which penalizes the accuracy of calculated duct Mach numbers by an unknown amount. The error in measuring compressor speed is within 50 revolutions per minute. Normalized air-flow rate is estimated to be accurate to about 2 lb/sec. This parameter was determined from unpublished results of engine tests by the NACA Lewis Laboratory. The accuracy of free-stream Mach number is within ±0.01 at the lower speeds and ±0.02 between $M = 0.9$ and 1.0. At supersonic speeds the error in Mach number should be very small, depending on instrument error only.

TESTS

The data reported in this paper represent pull-ups, speed runs, turns, and sideslips. Altitude ranged from 33,000 to 50,000 feet with most of the data obtained at an altitude of 40,000 feet. Mach number varied from about 0.6 to 1.1.

It was found that the induction system-engine combination had very low throttle-fixed surge incidence at the altitudes normally reached by the airplane. In order to reach the altitudes where the probability of surge increased, it was necessary to resort to a special maneuver consisting of a level run at about 45,000 feet to provide momentum, followed by a fixed-throttle pull-up which allowed the airplane to "zoom" to about 50,000 feet. About half these maneuvers provided surge. Four of these throttle-fixed surges were recorded along with five other surges

recorded under unknown throttle conditions. The nine surges recorded are included in this paper with the conditions of their occurrence for comparison with conditions where no surge was encountered.

DISCUSSION OF RESULTS

Although intercompressor and compressor discharge instrumentation was not available for all surges encountered, three of the throttle-fixed surges were recorded with total-pressure probes at stations 4 and 5. According to NACA Lewis altitude wind-tunnel data for a similar engine, the compression ratio value prior to surge across the low-speed compressor is well within the steady-state operating region. However, the compression ratio value between stations 4 and 5 (across the high-speed compressor) is sufficient to initiate surge within the high-speed compressor.

The relationship of compressor face total pressure with high-speed compressor velocity prior to surge is shown in figure 5. As can be seen, the region where surge was encountered is limited to a very small part of the region of total flight experience; that is, the region where compressor face total pressure is less than 400 pounds per square foot. The coarse cross-hatched area indicates the part of the flight experience region where high-speed compressor surge was encountered for a similar engine at the NACA Lewis Laboratory.

Although the region of flight experience is quite extensive, it can be seen that throttle-fixed surge was not encountered in flight until the conditions were the same as those existing for high-speed compressor surge in the wind tunnel. Even for the surges where the throttle condition is unknown the occurrence is within or close to those conditions for high-speed compressor surge in the tunnel. Therefore, because these conditions for surge in flight and in the tunnel are similar and because the air flow to the engine in the tunnel was undistorted, it is believed that the surges encountered during flight are not induced by compressor face distortion.

The contention that these surges are unrelated to distortion is substantiated by figure 6 where the distortion factor Δ_{av} is related to mass-flow ratio, angle of attack, and normalized air-flow rate. This figure shows conditions existing at the compressor face for surge-free operation (open symbols) and conditions prior to surge (solid symbols). The distortion prior to surge is no greater; in fact, it is usually less than the distortion for surge-free operation. As can be seen, there is nothing unique about surge occurrence relative to distortion and the other parameters shown.

Each of the next two figures, 7 and 8, illustrates the circumferential and radial pressure-recovery profiles at the compressor face. The solid symbols represent the average pressure recovery of each survey rake at the circumferential position of the rake. The connected straight lines within the radial segment r form the radial profile for each rake. The solid horizontal line represents the overall mean pressure recovery and the dashed line illustrates the circumferential deviation (distortion) from the overall mean recovery.

Figure 7 shows the compressor face recovery profiles immediately prior to the four surges encountered with fixed throttle. Pressure profiles cannot be shown during the surges because the dynamic response of the instrumentation was not sufficient to follow the disturbance. It can be seen that the dashed fairing at $\theta = 150^\circ$ is near the same level as at $\theta = 210^\circ$. This fairing is supported by data obtained during tests when a rake was located at $\theta = 150^\circ$ (fig. 8(b)).

The pattern follows the conventional form for an installation of this type, showing low recovery at the top (0° or 360°) and even lower at the bottom (180°). At about 30° from the bottom the radial profile loses the usual inverted "U" shape associated with fluid flow in pipes. However, this feature is associated not only with compressor-surge profiles but is also characteristic of this installation for normal-flight conditions as shown in figure 8.

Figure 8 is a presentation of the same type as shown in the preceding figure. These data represent turns, speed runs, and sideslips without compressor surge. These maneuvers reveal generally low total-pressure recovery at the compressor face with a high level of distortion. Comparison of these profiles will also show that distortion is not related to angle of attack, Mach number, or sideslip for the range of these tests. A possible explanation of the insensitivity of compressor face distortion to these external parameters is that the effective diffuser expansion angle is so small (about 1°) that distortion originating near the inlet dissipates through natural mixing before reaching the compressor. Hence the distortion which is experienced should be a function of the duct internal geometry and internal air-flow parameters. The dependence of distortion on the latter factor is demonstrated in figure 6 in which the relationship of distortion to normalized air-flow rate is shown.

Much of the data of figure 8 are shown in figure 9 by comparing the effect of angle of attack or sideslip on pressure recovery, distortion, and various duct and engine parameters. Figure 9(a) represents a turn at about 40,000 feet, $M \approx 0.84$, and a nearly constant normalized air-flow rate of about 182 pounds per second. The pressure-recovery values for stations 1, 2, and 3 are nearly parallel, indicating that the duct internal losses are independent of angle of attack and that the lip

losses, represented by station 1, increase rapidly with angle of attack. The pressure-recovery loss at the compressor face between angles of attack of 4° and 10° is about 0.06. In addition, the former observation that distortion at the compressor face is not affected by angle of attack is verified.

Figure 9(b) shows a similar plot for two speed runs which varied in Mach number from 0.6 to almost 1.0, while altitude and the associated angle of attack varied over a range comparable to the preceding turn (fig. 9(a)). The relationship of pressure recovery to free-stream Mach number can be seen by the reduced slope of the pressure-recovery curve for these maneuvers. Here the loss in compressor face recovery between angles of attack of 4° and 10° is about 0.03 (half the value of fig. 9(a)). In addition, distortion is little affected by Mach number, especially distortion factor Δ_{av}. The duct Mach numbers display the same trends during the speed runs as during the turn at constant Mach number and are only slightly influenced by angle of attack.

A similar presentation is made in figure 9(c) for dive-recovery data at $M \geqq 1.0$. Here, again, duct Mach number and distortion show only slight changes with increasing angle of attack; however, the pressure-recovery loss from an angle of attack of 4° to 10° is about 0.10, indicating a more severe lip loss with angle of attack at Mach numbers in excess of 1.0.

A similar comparison is presented in figure 9(d) to show the effect of sideslip at constant angle of attack. For the range of sideslip shown, the pressure recovery and distortion are independent of sideslip.

The comparisons made in figure 9 show graphically the manner in which the inlet lip, angle of attack, internal losses, and supersonic speed affect the pressure recovery of this installation. However, an attempt to relate pressure recovery to a flow-rate parameter in flight is not as conclusive, as can be seen in figure 10. The variation of pressure recovery with several air-flow parameters is shown, although the more commonly used normalized air-flow rate is probably the most intelligible.

For the data at an angle of attack of 4° the existence of a sudden increase in recovery loss with increase in normalized air flow is especially apparent. This trend is normal for inlet ducts as choking is approached; however, most maneuvers should obviously be flown at air-flow rates low enough to avoid the "knee" in the curve. Flight experience with the YF-102 airplane has shown that for most maneuvers the normalized air-flow rate is beyond this "knee," which accounts for the generally low pressure recovery of this duct-engine combination.

This condition is illustrated in more detail in figure 11 where flight data are compared with recovery characteristics and the choking boundary, both of which are estimated in reference 2. Sensing devices were not available at the proper locations to indicate positively a choked condition in this duct. However, in view of the trend of flight pressure-recovery values and the position of the flight-recovery values relative to the estimated choking line, it is thought that a choked condition existed for most flight conditions. This is a rather serious case of mismatching.

During these tests it was observed that as angle of attack increases, the compressor face survey rakes at $\theta = 90^\circ$ and $\theta = 270^\circ$ experience different total-pressure values. Although an extensive study has not been made, four special maneuvers were recorded at Mach numbers between 0.75 and 0.85 with only the rakes at $\theta = 90^\circ$ and 270° installed at the compressor face. Rakes at stations 1 and 2 were also removed to prevent their presence from influencing the results. These data, presented in figure 12, show a significant and repeatable total-head differential between the right and left sides of the compressor face at angles of attack above 11°. As can be seen, the differential changes sign near an angle of attack of 15°.

CONCLUDING REMARKS

The combination of the YF-102 airplane and a two-spool turbojet engine has been found to display the following characteristics:

1. The combination had a very low compressor-surge incidence for normal-flight operations.

2. For the recorded compressor surges there appears to be no relationship between compressor face distortion and surge.

3. For the range of these tests, distortion is not related to angle of attack, sideslip, or free-stream Mach number. This probably is due to the natural mixing associated with the low expansion angle diffuser. There is a relationship between distortion and normalized air-flow rate, however.

4. The duct-engine system is mismatched for most flight conditions, resulting in high internal losses. These losses are unaffected by angle of attack or free-stream Mach number. The inlet-lip losses increase rapidly with angle of attack and this increase in loss with angle of attack is greatly aggravated when Mach number exceeds 1.0.

5. The total-pressure variation with angle of attack for the YF-102 twin-side inlet system is not the same on both sides for negligible sideslip angles and varies in a repeatable manner with angle of attack.

High-Speed Flight Station,
National Advisory Committee for Aeronautics,
Edwards, Calif., March 12, 1957.

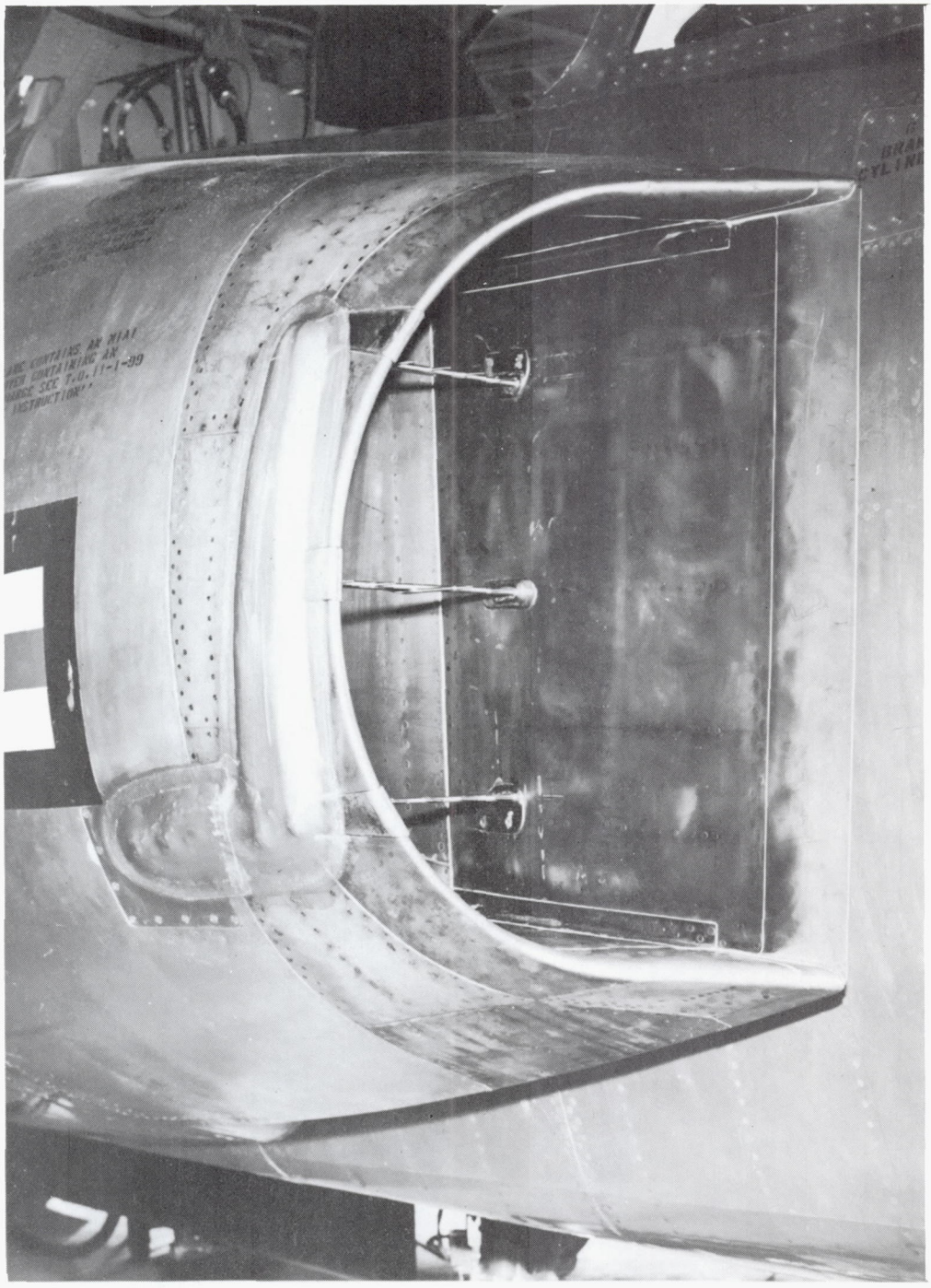
REFERENCES

1. Saltzman, Edwin J., Bellman, Donald R., and Musialowski, Norman T.: Flight-Determined Transonic Lift and Drag Characteristics of the YF-102 Airplane With Two Wing Configurations. NACA RM H56E08, 1956.

2. Nakamura, H., and Tsunoda, W.: Thrust Available and Engine Air Inlet Performance of the F-102 Airplane. Rep. ZJ-8-002 (Contract No. AF-33(600) 5942), Consolidated Vultee Aircraft Corp., Nov. 24, 1952.

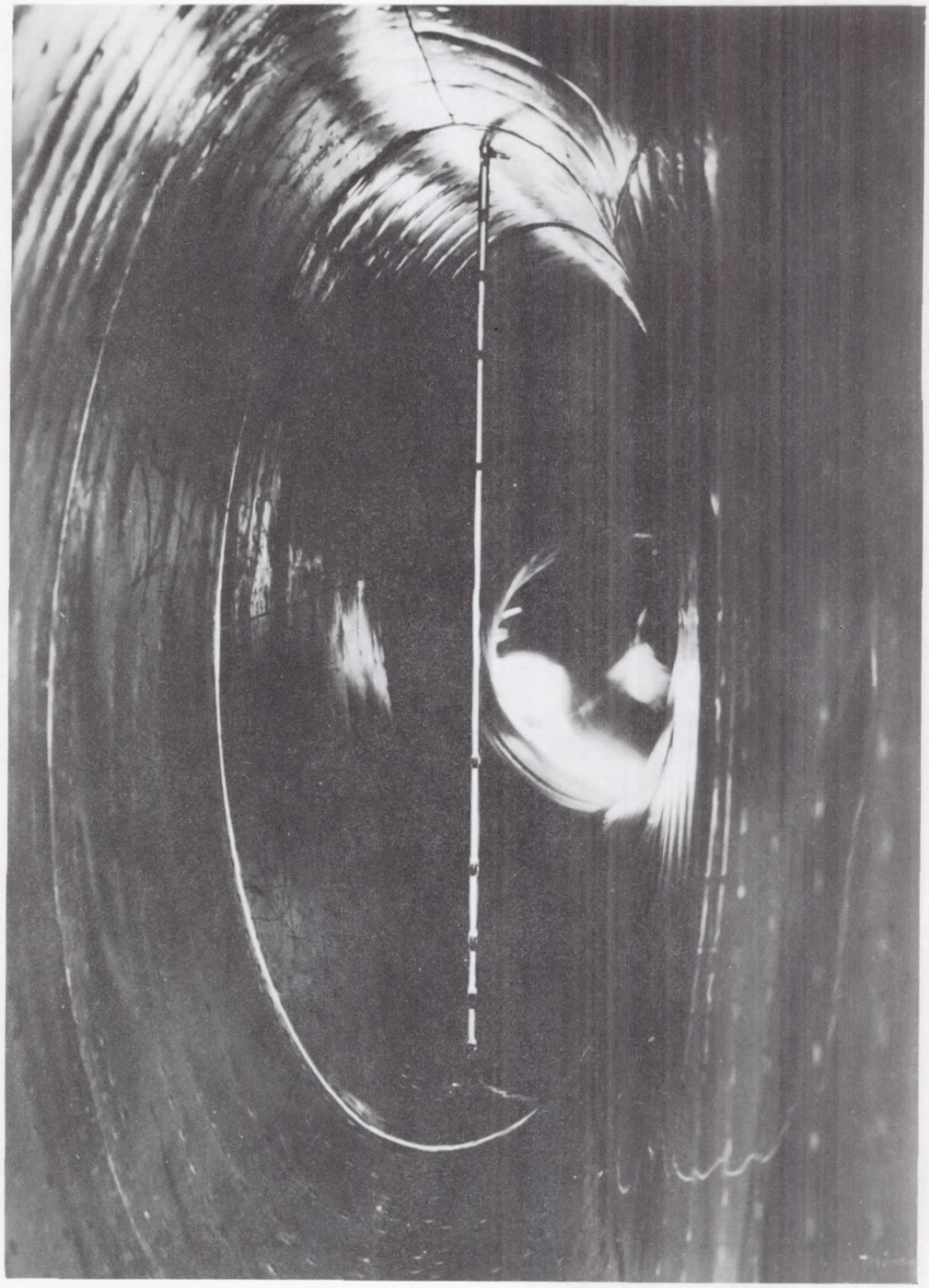


Figure 1.- General view of YF-102 airplane showing inlet. L-57-182



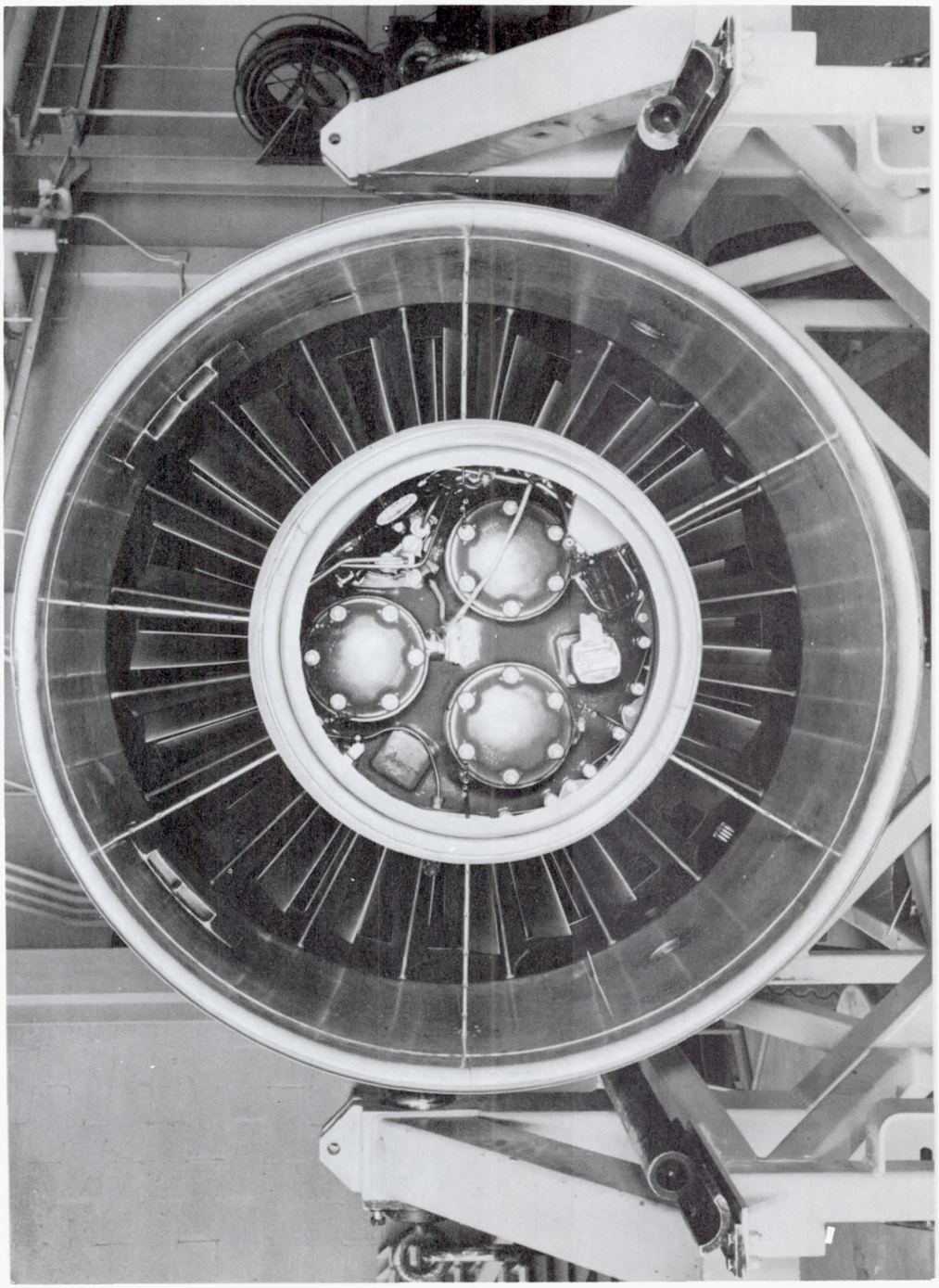
(a) Station 1. E-1568

Figure 2.- Photographs of survey stations.



(b) Station 2. E-1761

Figure 2.- Continued.



E-1584

(c) Station 3.

Figure 2.- Concluded.

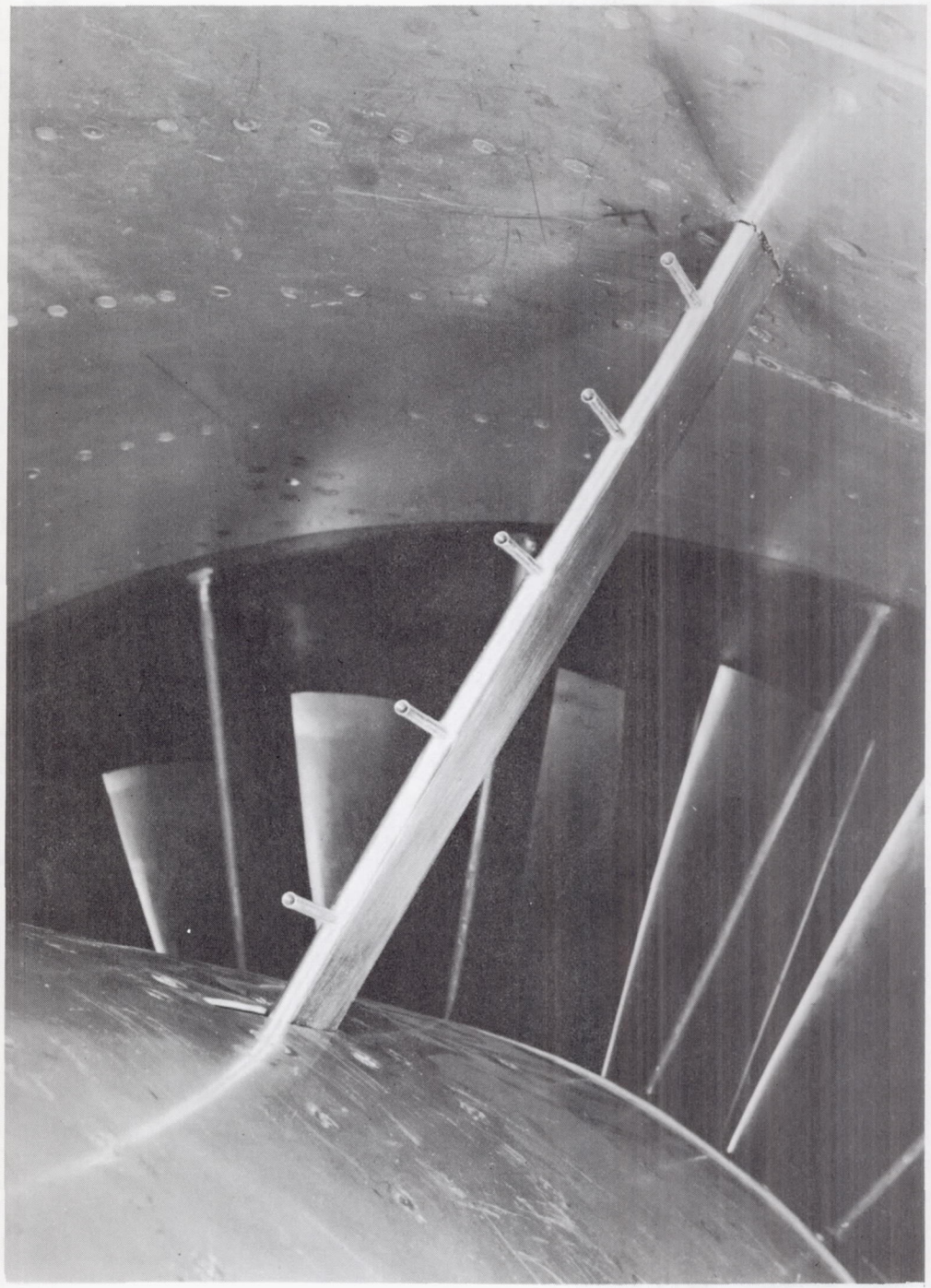
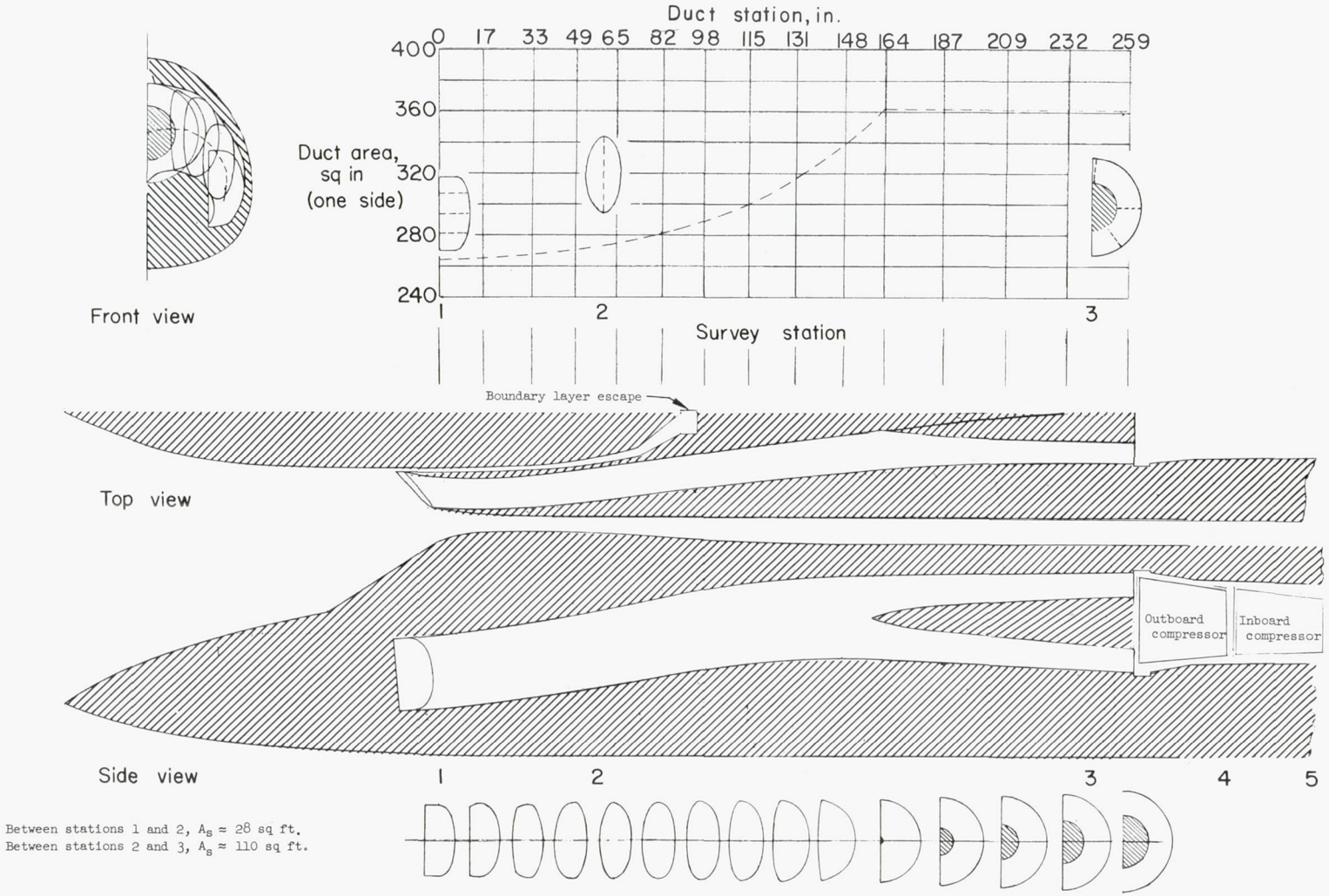
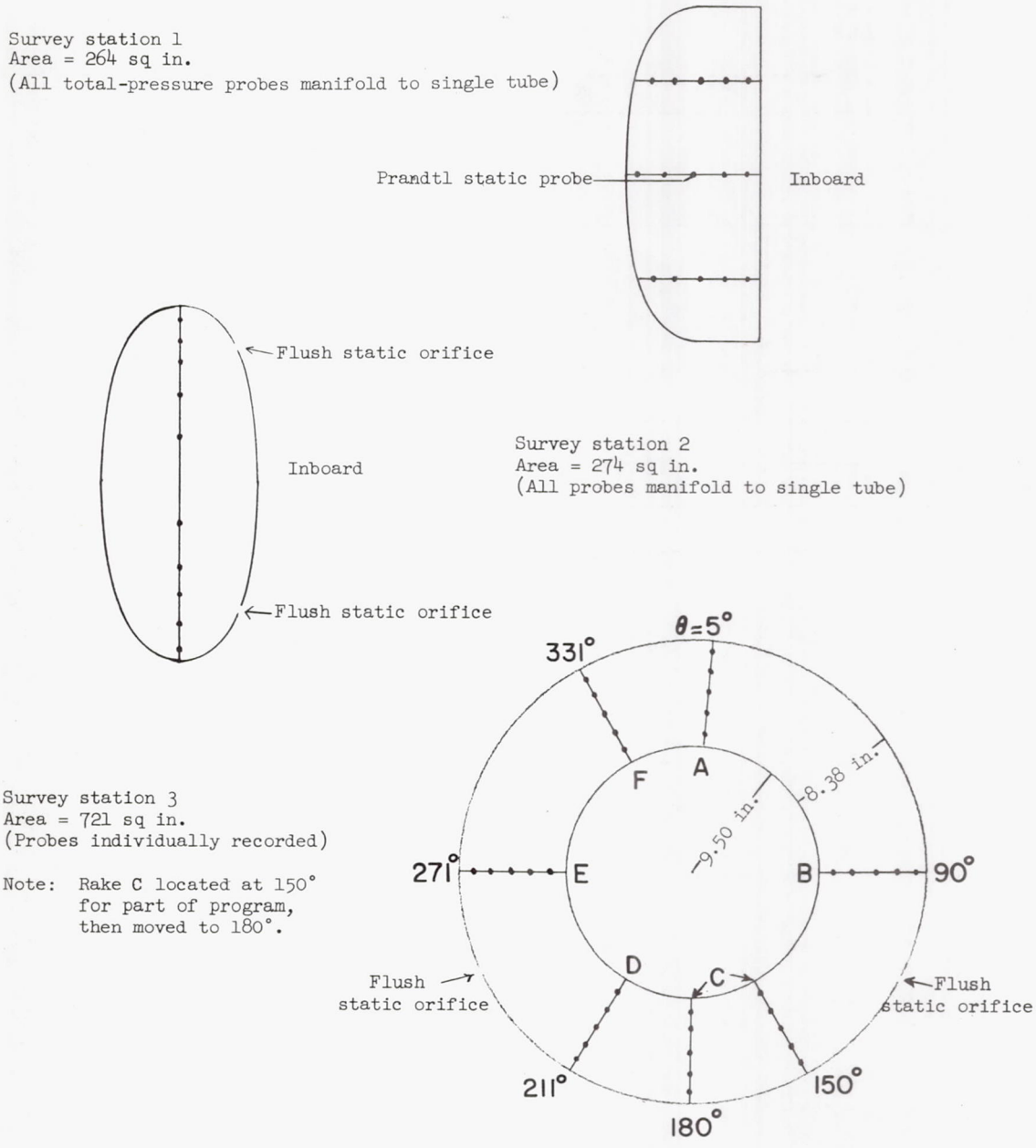


Figure 3.- Close-up view of survey rake at station 3. E-1585



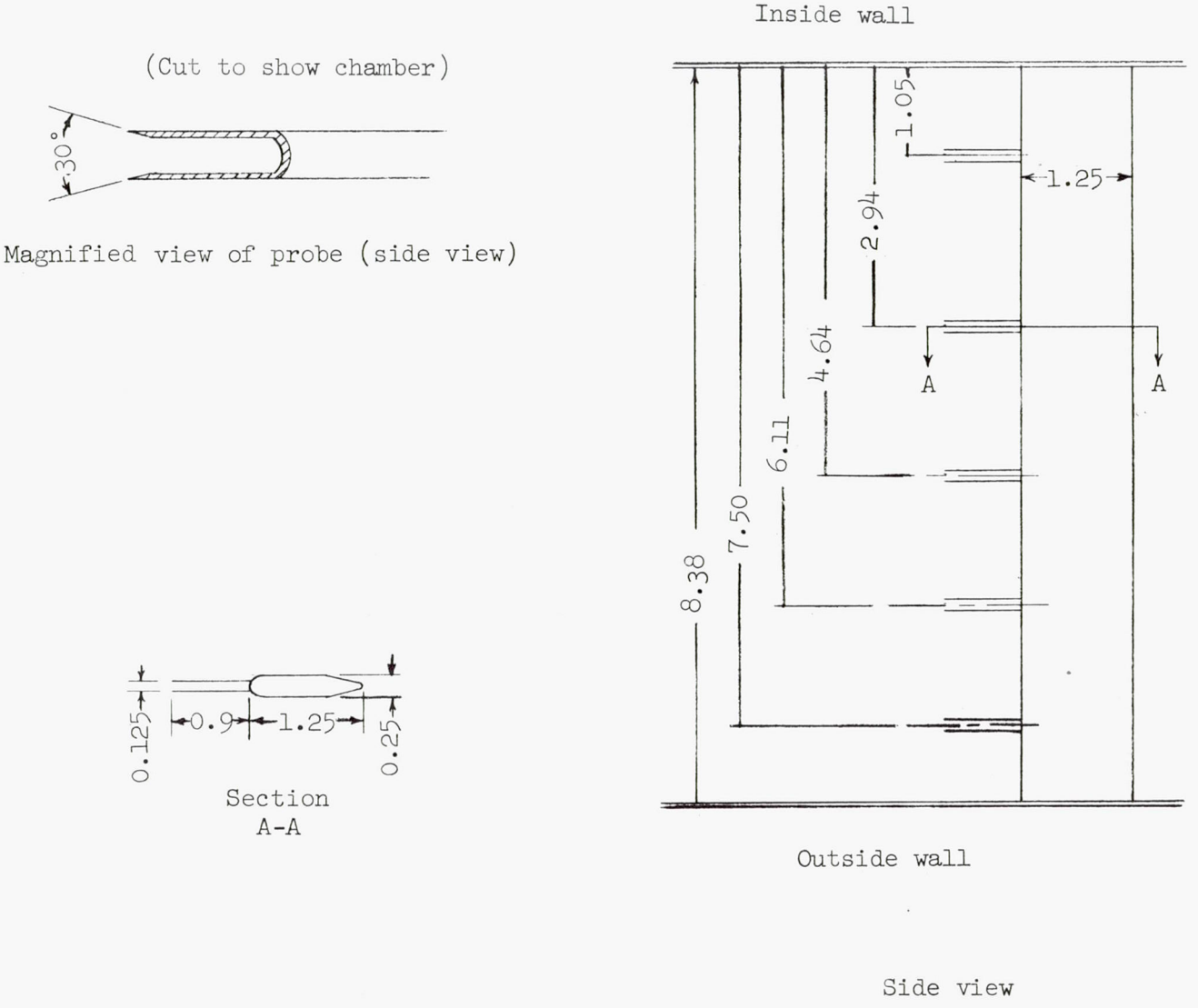
(a) Location of survey stations.

Figure 4.- Physical details pertaining to the survey stations.



(b) Front view of survey station profiles.

Figure 4.- Continued.



(c) Details of rakes at station 3. All dimensions in inches.

Figure 4.- Concluded.

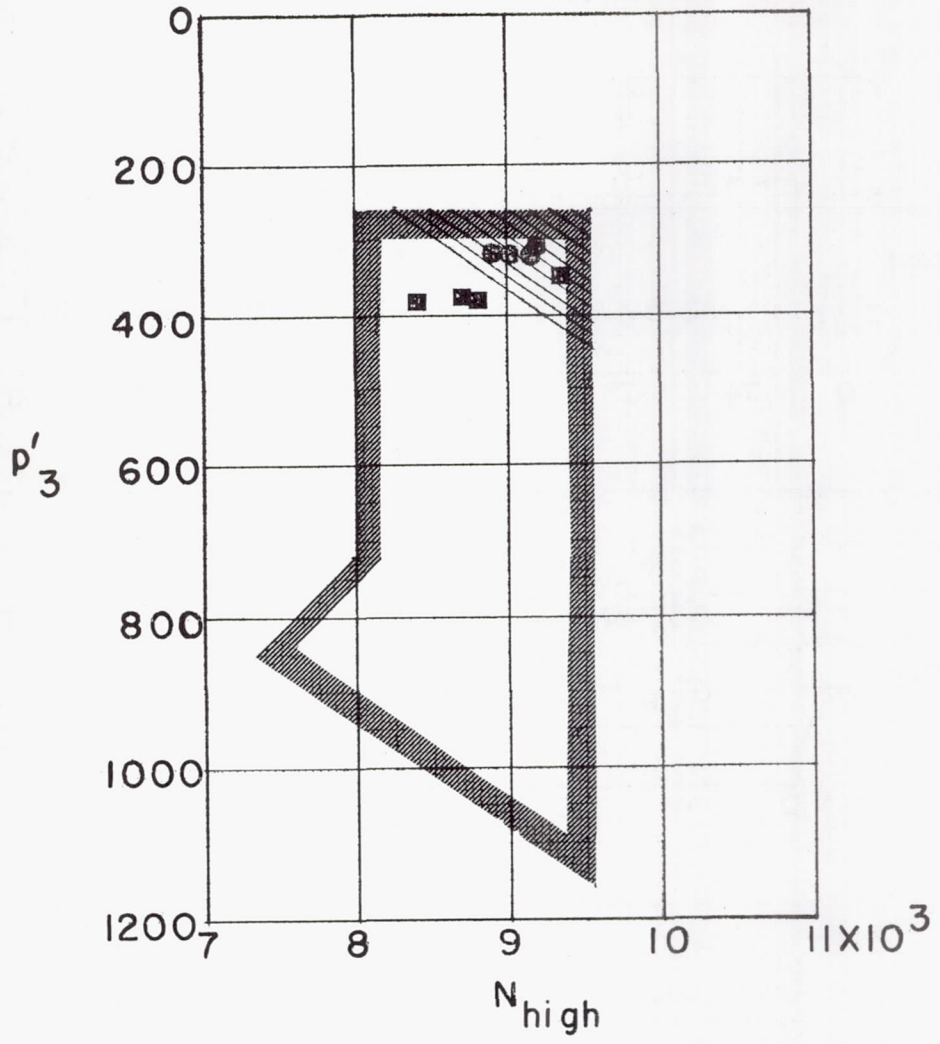


Figure 5.- Comparison of surge conditions during flight with those for a similar engine tested at the NACA Lewis Laboratory.

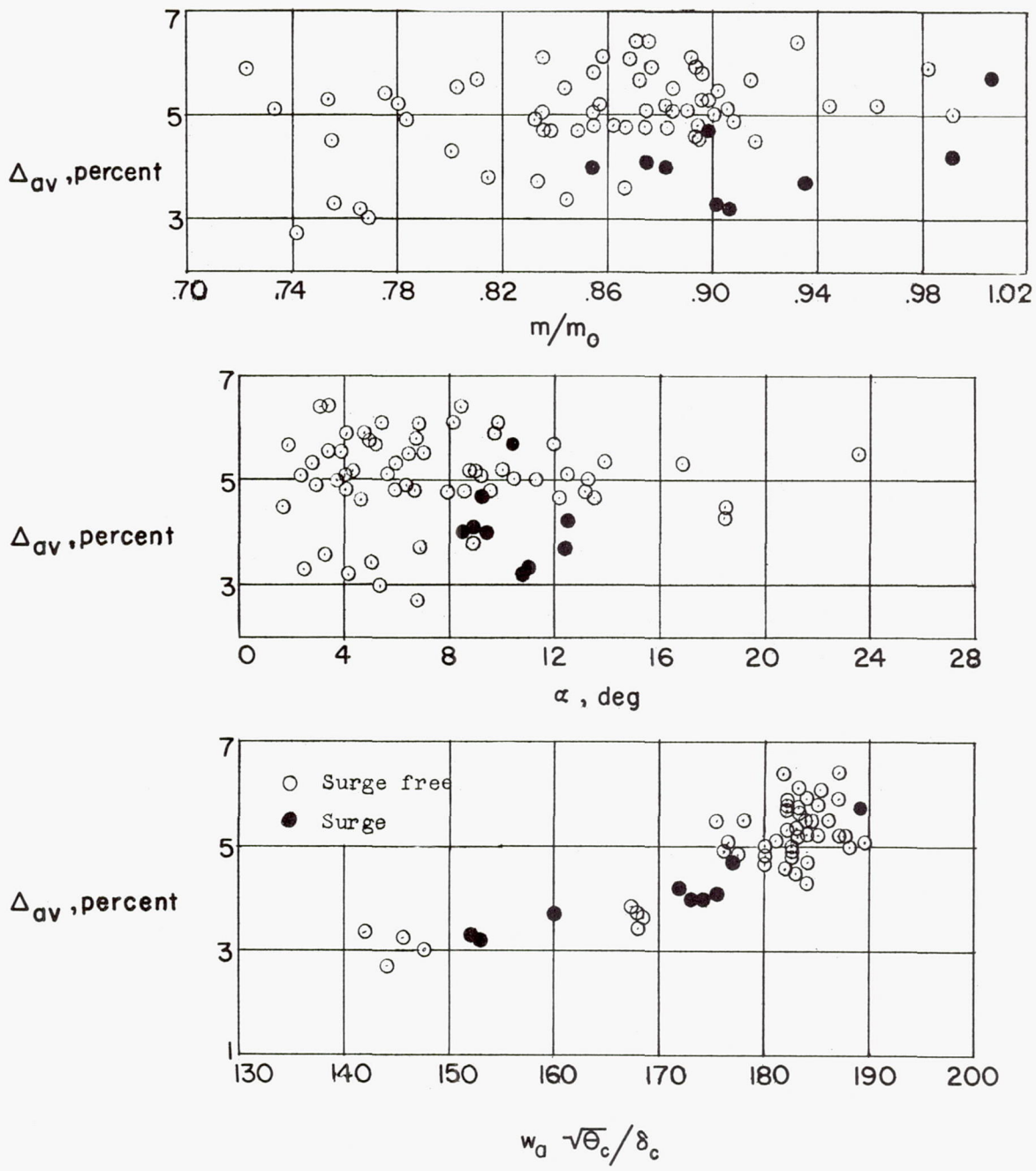


Figure 6.- Relative distortion for surge-free and surge operation, and relationship of distortion to m/m_0, α, and $w_a\sqrt{\theta_c}/\delta_c$.

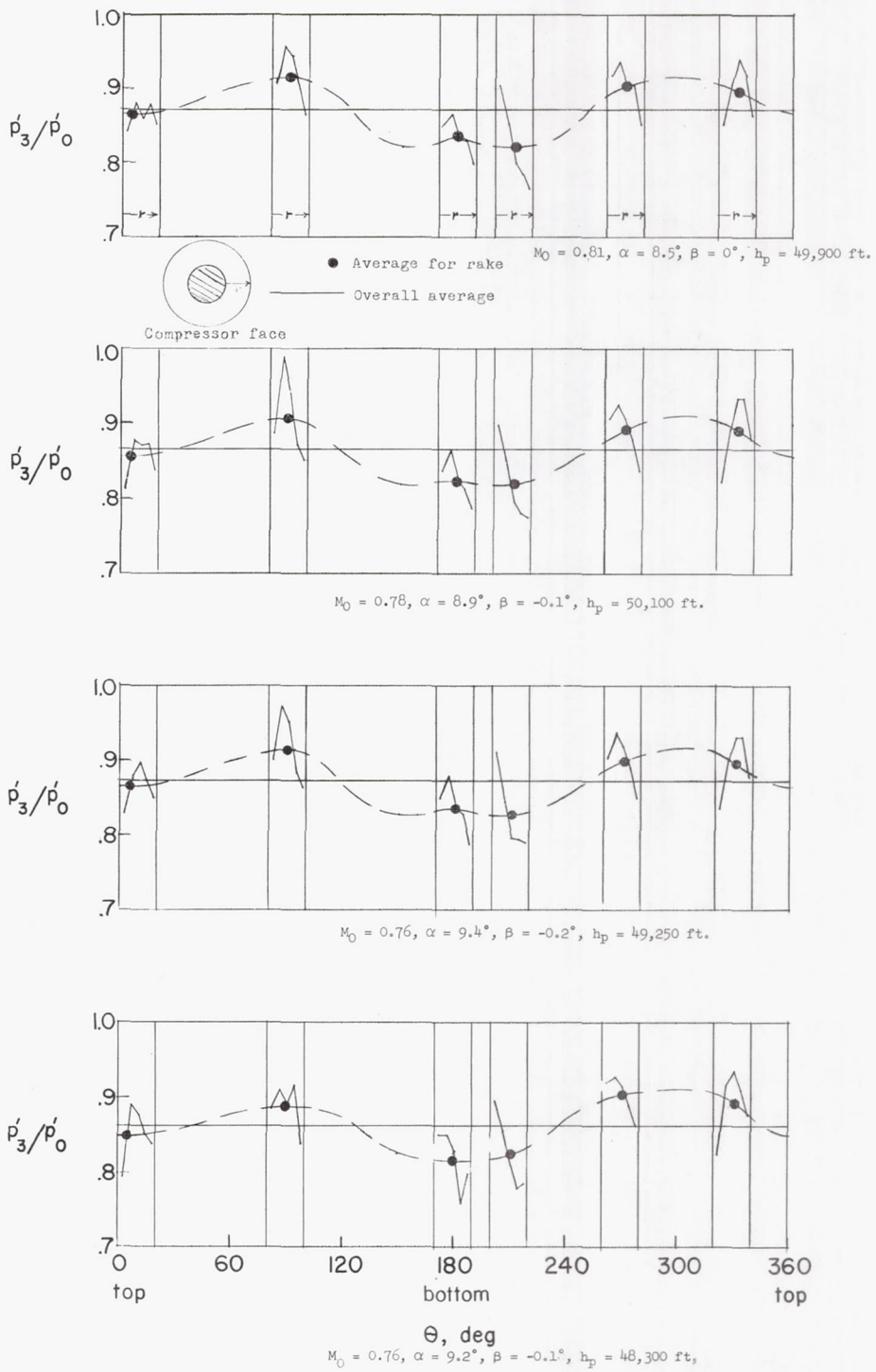
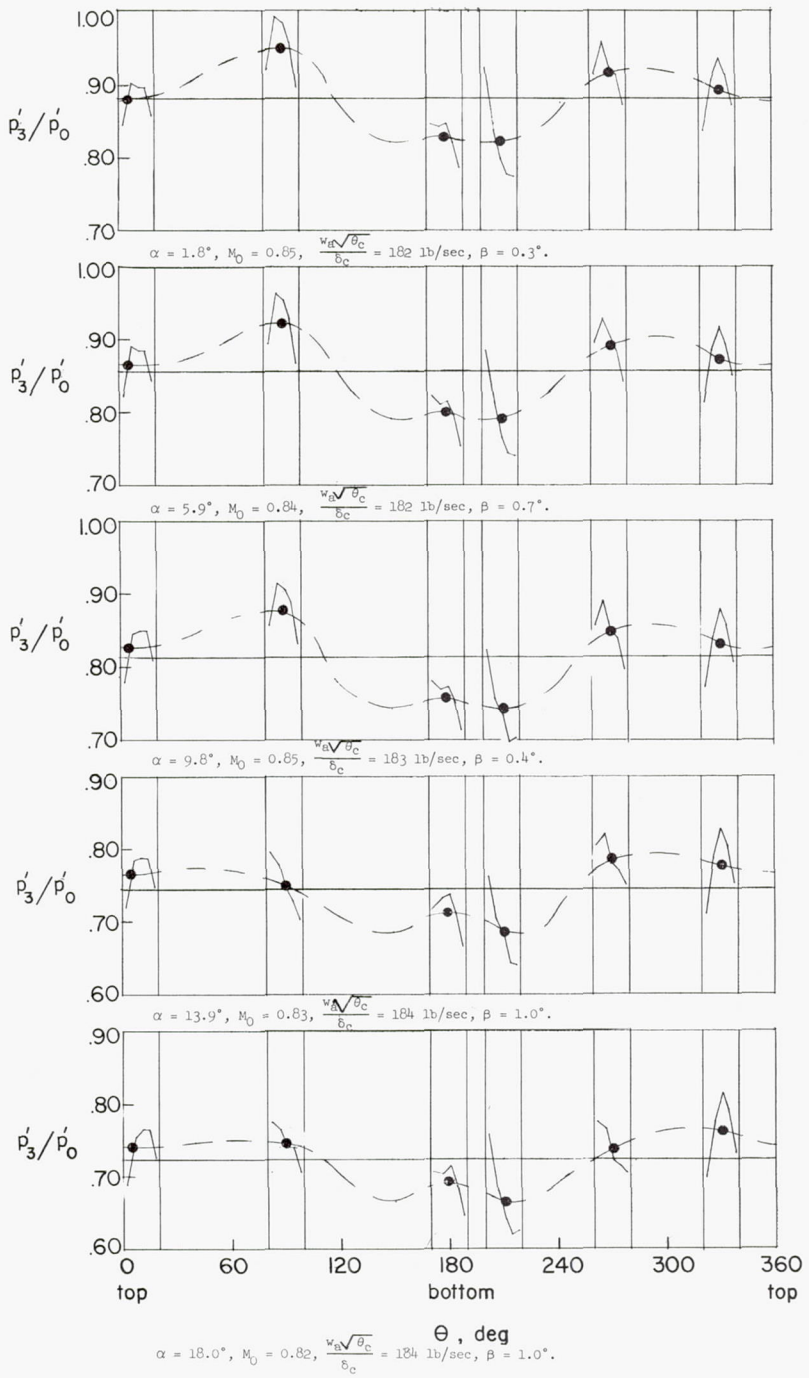
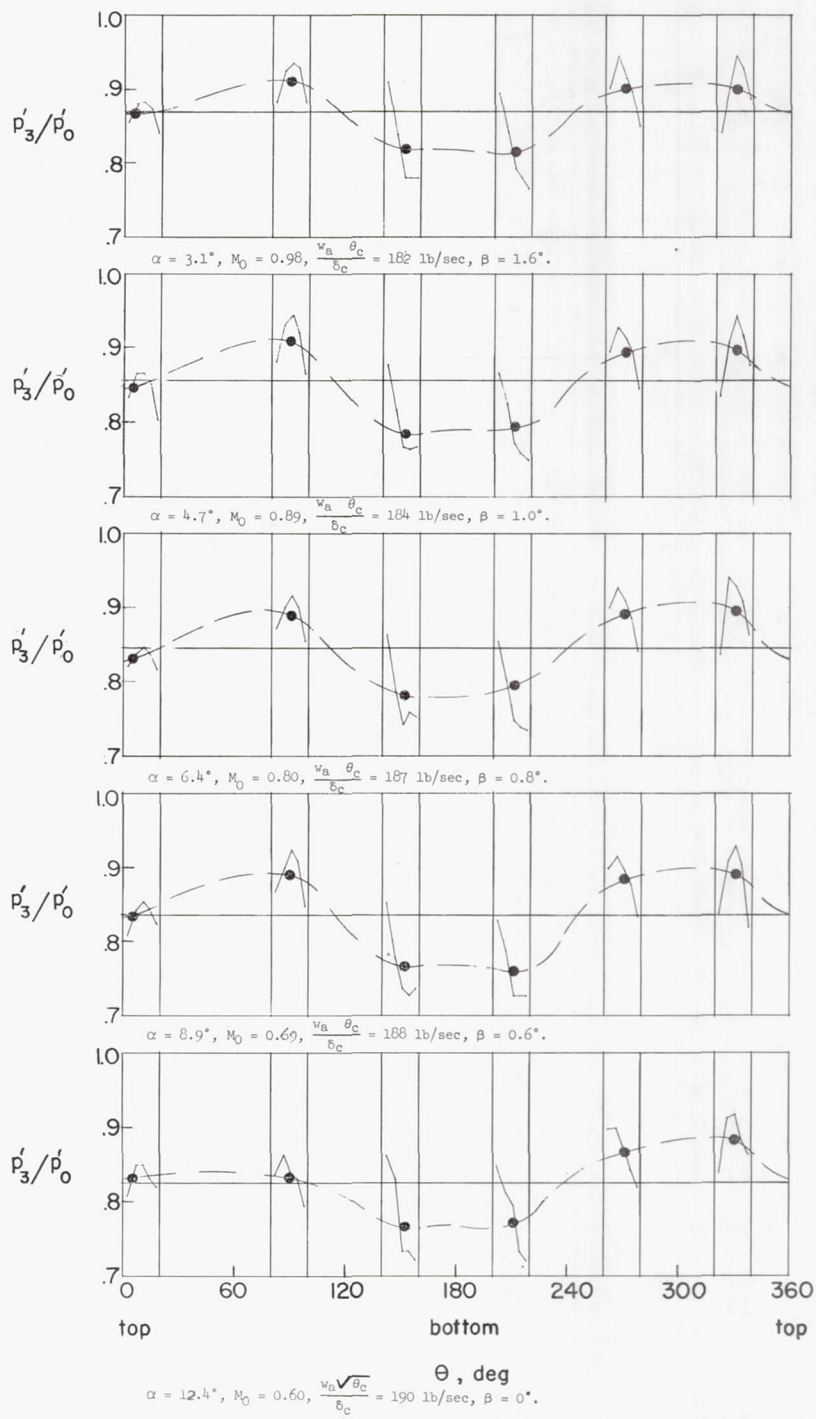


Figure 7.- Compressor face recovery profile prior to each of four throttle-fixed surges.



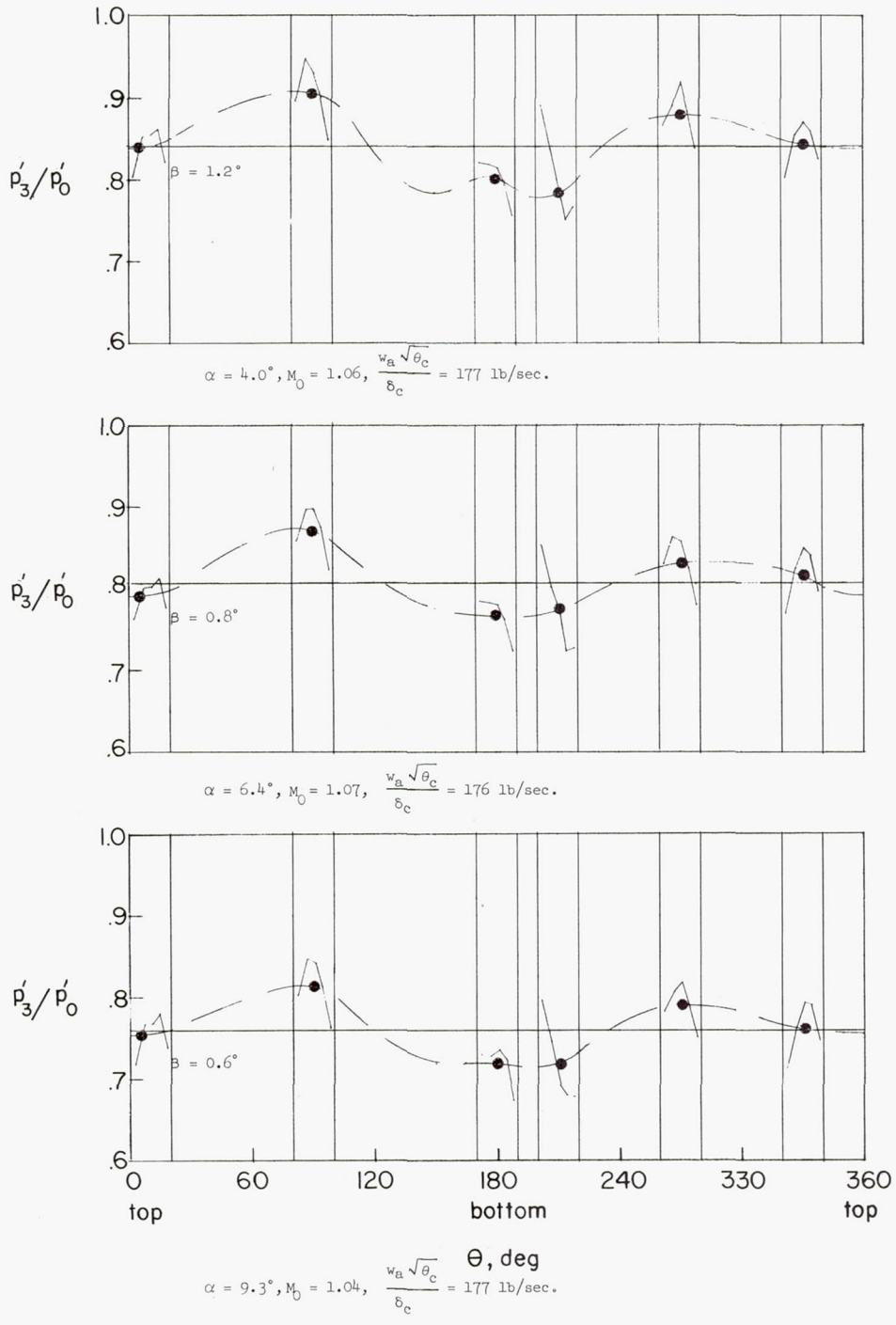
(a) Subsonic turn at constant Mach number, $h_p \approx 41{,}000$ feet.

Figure 8.- Circumferential and radial variation of pressure recovery during several maneuvers.



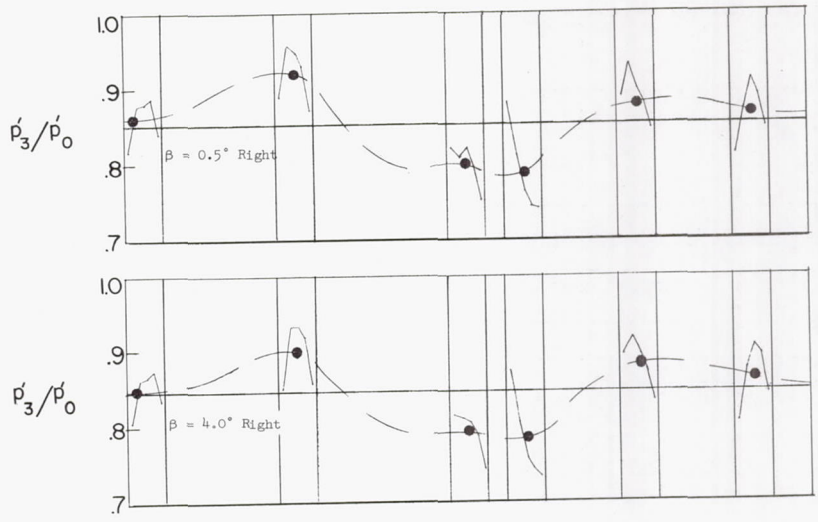
(b) Speed run from M = 0.6 to M ≈ 1.0; $h_p \approx$ 44,000 to 41,000 feet.

Figure 8.- Continued.

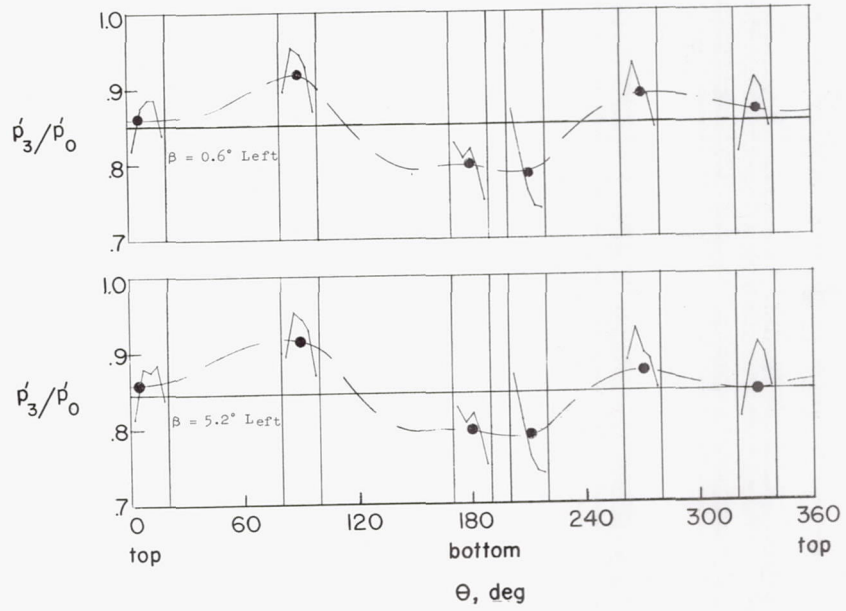


(c) Supersonic dive recovery, $h_p \approx$ 38,000 to 37,000 feet.

Figure 8.- Continued.

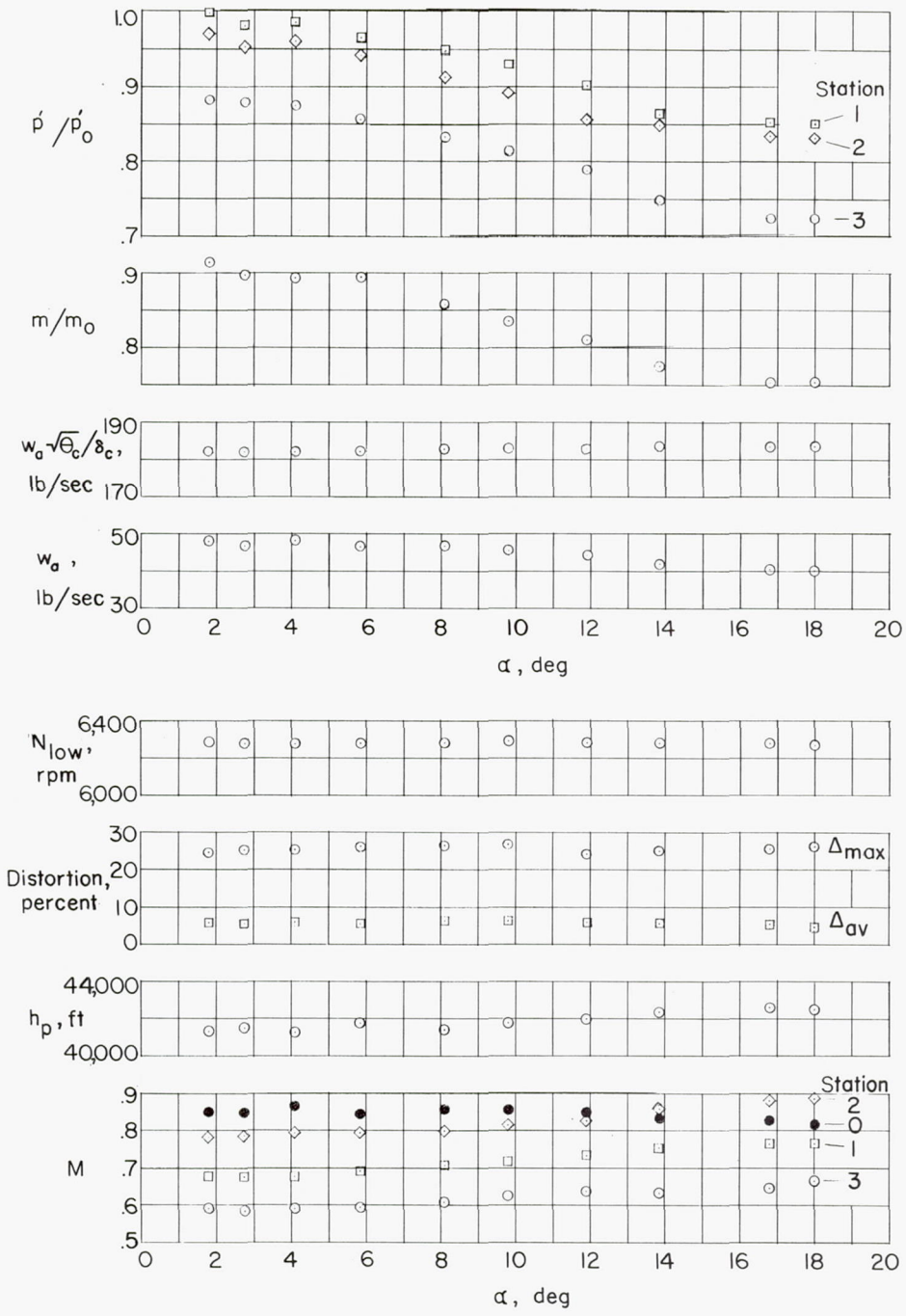


(d) Right sideslip, $\alpha \approx 6.0°$, $M_0 \approx 0.85$, $\frac{w_a\sqrt{\theta_c}}{\delta_c} = 183$ lb/sec, $h_p \approx 41{,}000$ feet.



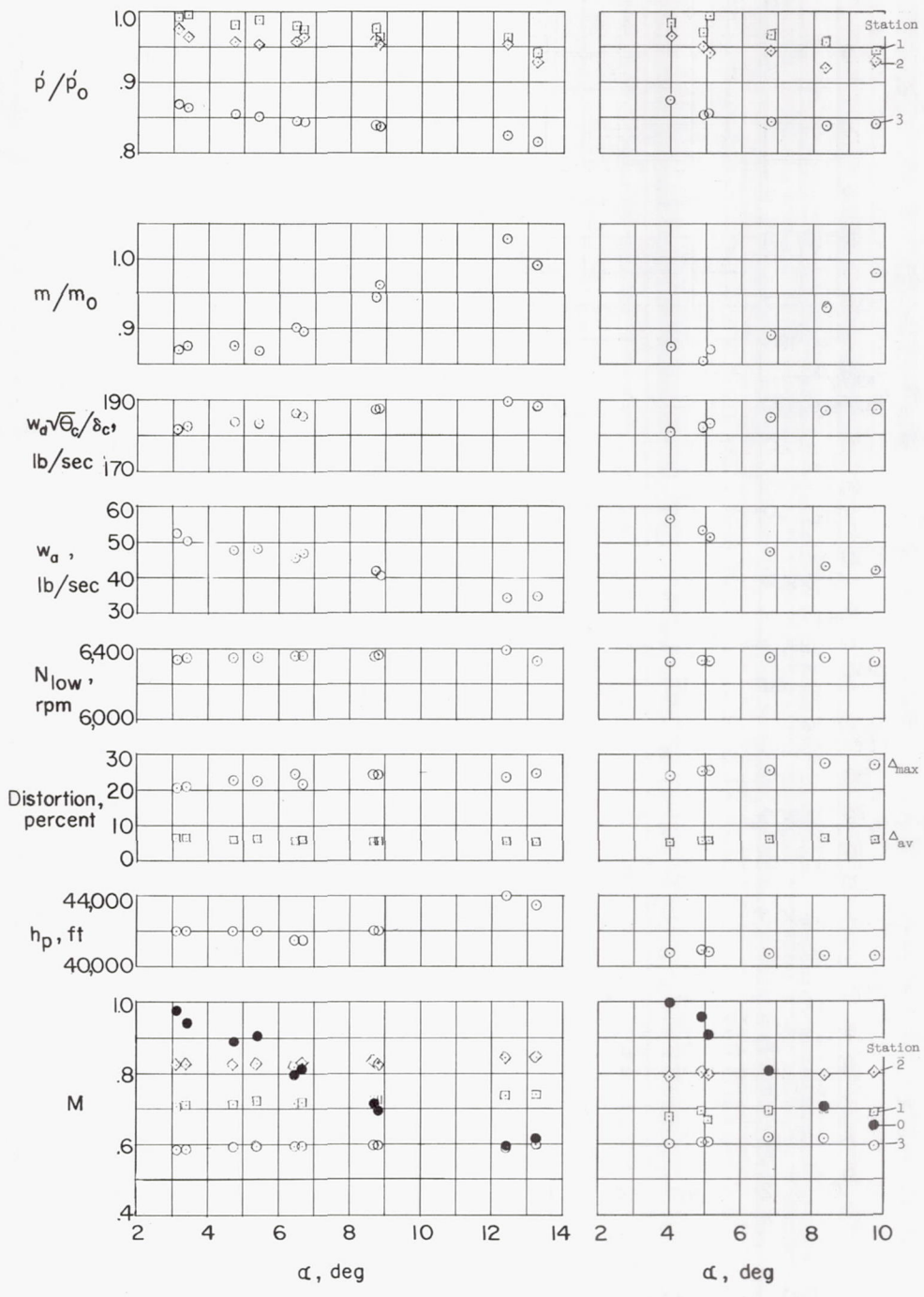
(e) Left sideslip, $\alpha \approx 6.0°$, $M_0 \approx 0.85$, $\frac{w_a\sqrt{\theta_c}}{\delta_c} = 183$ lb/sec, $h_p \approx 41{,}000$ feet.

Figure 8.- Concluded.



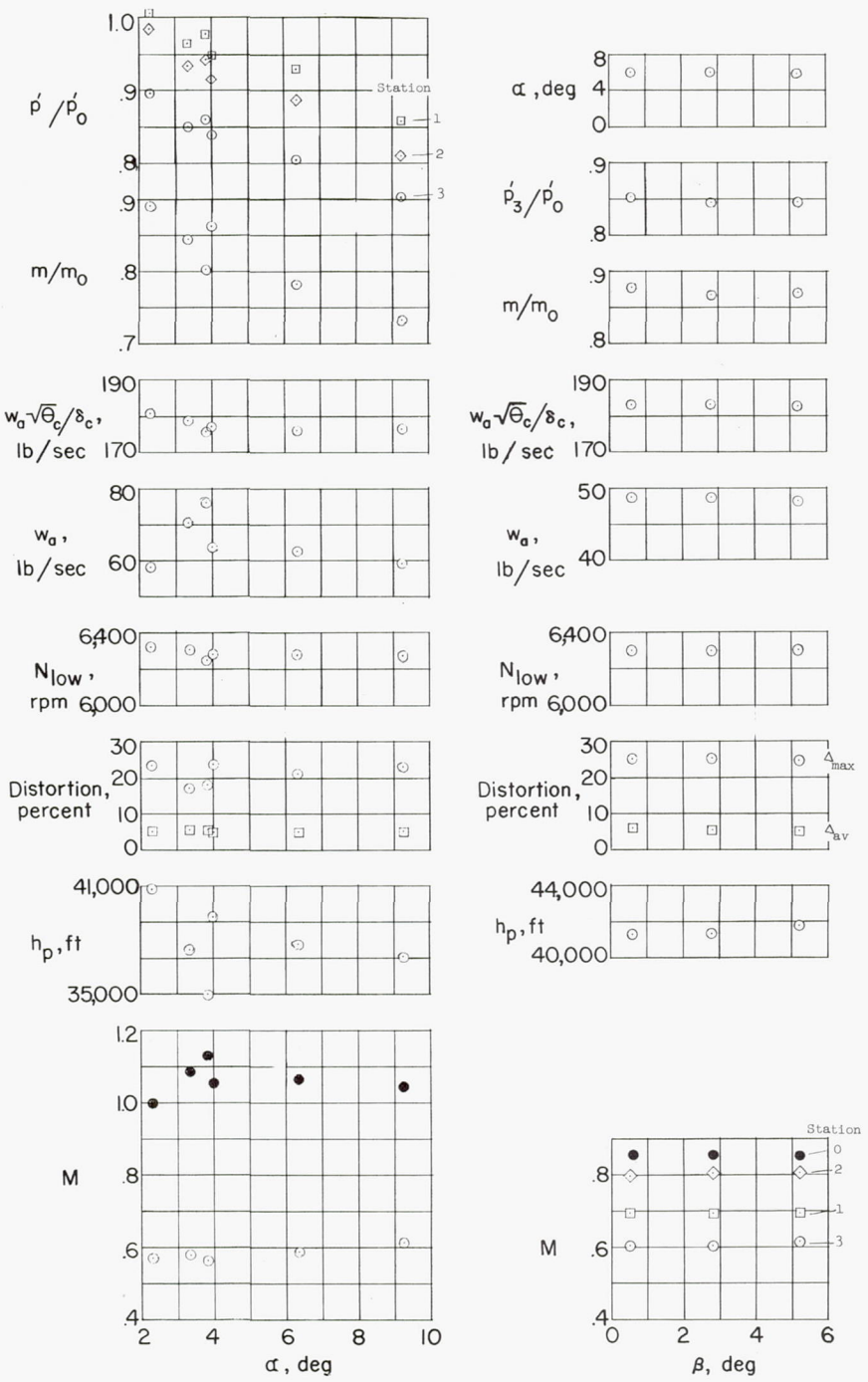
(a) Subsonic turn at constant Mach number.

Figure 9.- Variation with α and β of several induction system parameters.



(b) Speed runs from $M \approx 0.6$ to $M \approx 1.0$.

Figure 9.- Continued.



(c) Dive recovery data; $M \geqq 1.0$.

(d) Left sideslip.

Figure 9.- Concluded.

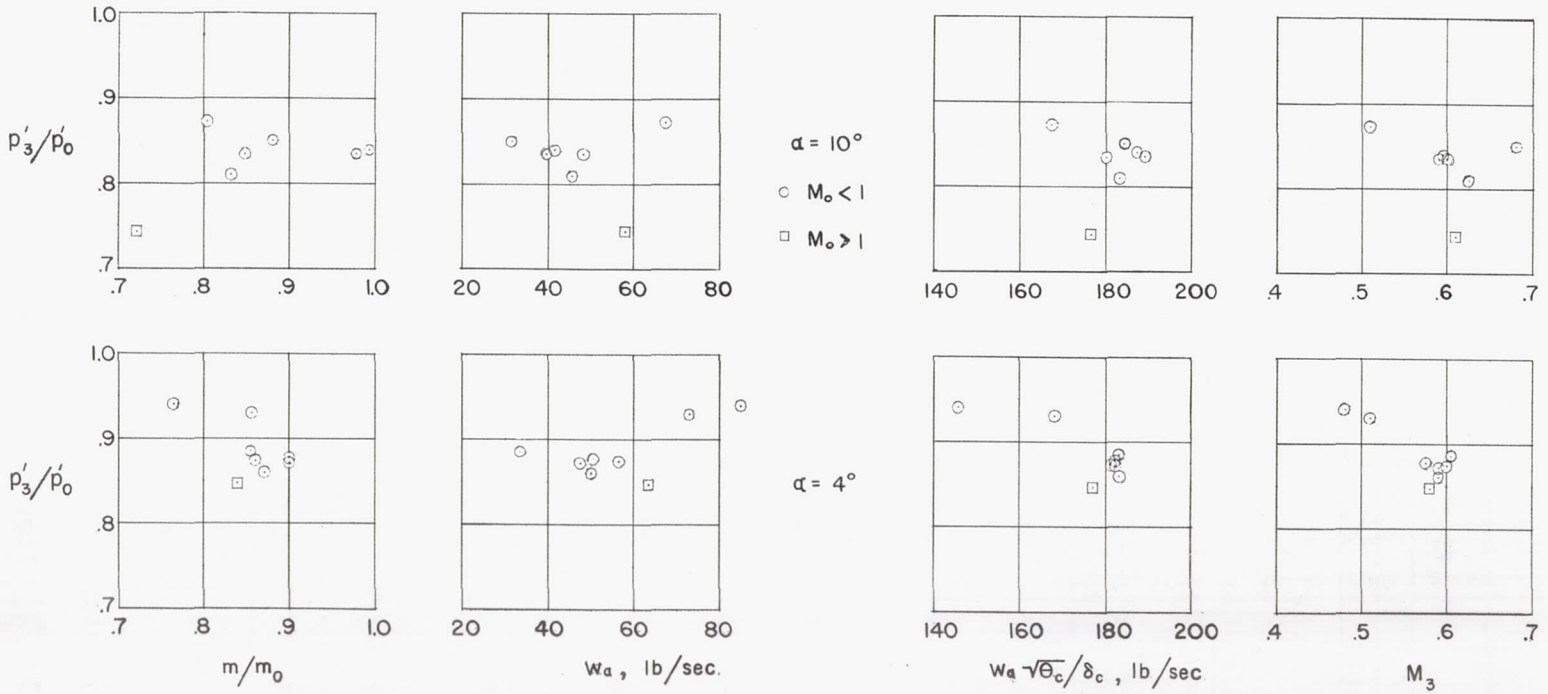


Figure 10.- Variation of pressure recovery at the compressor face with various flow-rate parameters for constant angle of attack.

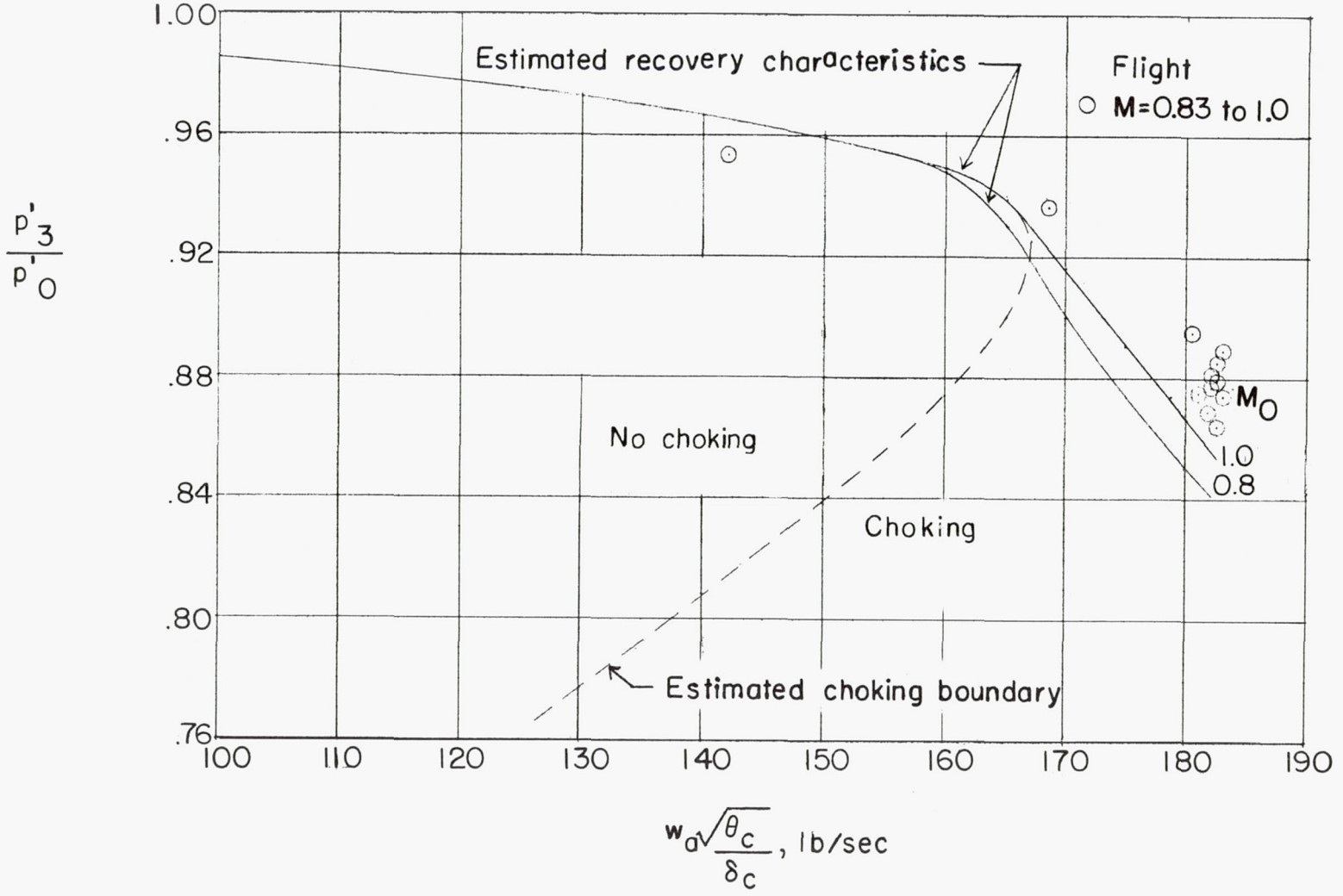


Figure 11.- Variation of compressor face pressure recovery with normalized air-flow rate.

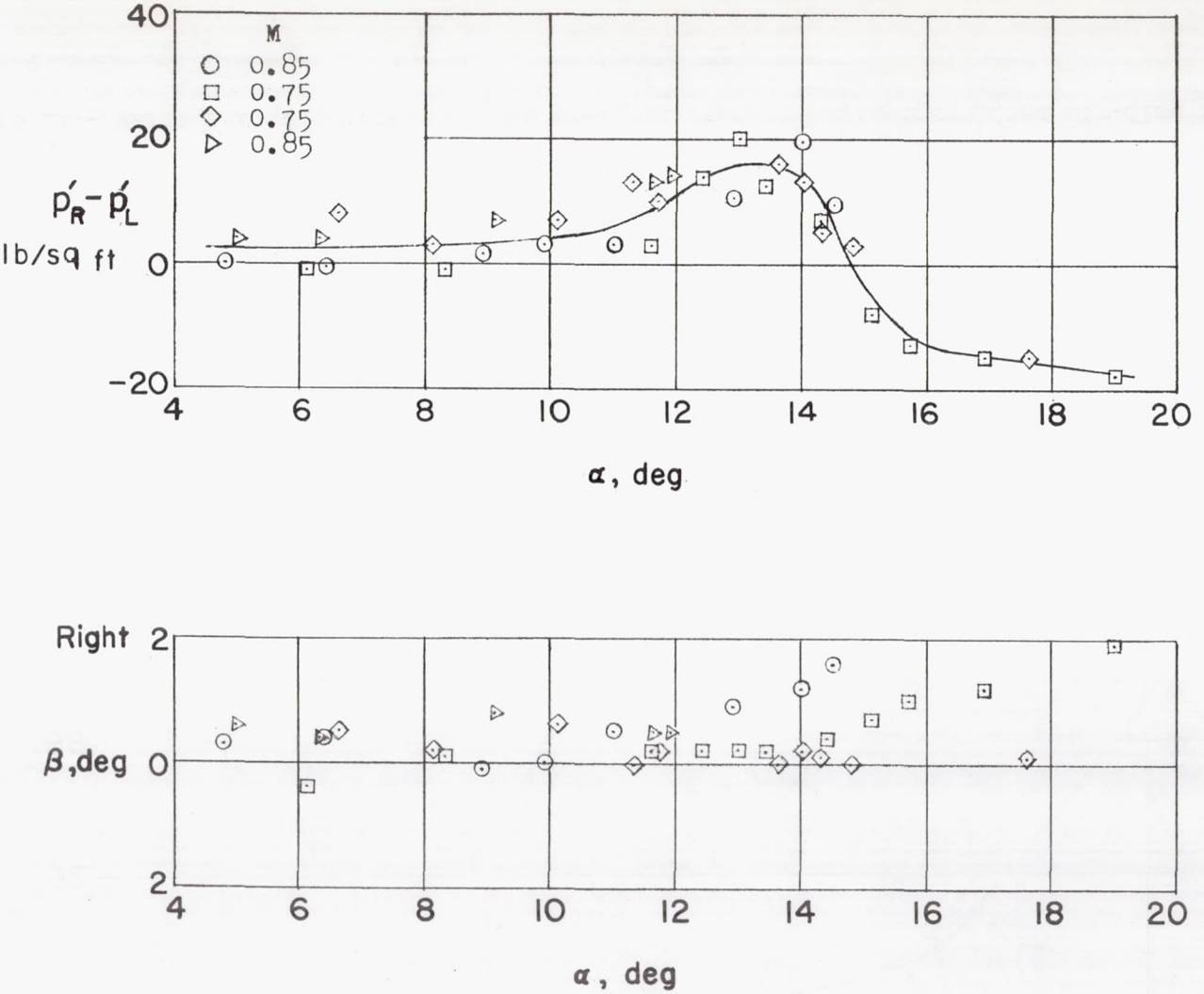
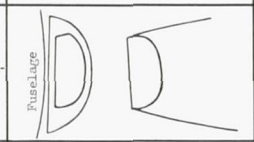
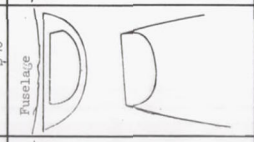


Figure 12.- Variation with angle of attack of differential pressure between right and left side of compressor face; $h_p \approx 40{,}000$ feet.

NOTES: (1) Reynolds number is based on the diameter of a circle with the same area as that of the capture area of the inlet.

(2) The symbol * denotes the occurrence of buzz.

Report and facility	Description			Test parameters				Test data				Performance		Remarks
	Configuration	Number of oblique shocks	Type of boundary-layer control	Free-stream Mach number	Reynolds number $\times 10^{-6}$	Angle of attack, deg	Angle of yaw, deg	Drag	Inlet-flow profile	Discharge-flow profile	Flow picture	Maximum total-pressure recovery	Mass-flow ratio	
CONFID. RM H57C22 NACA High-Speed Flight Station		Isen-tropic	Diverter	0.59 to 1.13	1.4 to 4.5	1 to 24	±5			X		X	0.72 to 1.01	In addition, there are included data pertaining to 1. Compressor stall 2. Compressor-face distortion 3. Engine-duct mismatching
CONFID. RM H57C22 NACA High-Speed Flight Station		Isen-tropic	Diverter	0.59 to 1.13	1.4 to 4.5	1 to 24	±5			X		X	0.72 to 1.01	In addition, there are included data pertaining to 1. Compressor stall 2. Compressor-face distortion 3. Engine-duct mismatching
CONFID. RM H57C22 NACA High-Speed Flight Station		Isen-tropic	Diverter	0.59 to 1.13	1.4 to 4.5	1 to 24	±5			X		X	0.72 to 1.01	In addition, there are included data pertaining to 1. Compressor stall 2. Compressor-face distortion 3. Engine-duct mismatching
CONFID. RM H57C22 NACA High-Speed Flight Station		Isen-tropic	Diverter	0.59 to 1.13	1.4 to 4.5	1 to 24	±5			X		X	0.72 to 1.01	In addition, there are included data pertaining to 1. Compressor stall 2. Compressor-face distortion 3. Engine-duct mismatching

Bibliography

These strips are provided for the convenience of the reader and can be removed from this report to compile a bibliography of NACA inlet reports. This page is being added only to inlet reports and is on a trial basis.

CONFIDENTIAL

CONFIDENTIAL